

# Synchrophasor-Based Real-Time Voltage Stability Index

Yanfeng Gong and Noel Schulz  
*Mississippi State University*

Armando Guzmán  
*Schweitzer Engineering Laboratories, Inc.*

Published in  
*Wide-Area Protection and Control Systems: A Collection of  
Technical Papers Representing Modern Solutions, 2017*

Previously presented at the  
2006 IEEE PES Power Systems Conference and Exposition, October 2006,  
and DistribuTECH Conference, February 2006

Originally presented at the  
32nd Annual Western Protective Relay Conference, October 2005

# Synchrophasor-Based Real-Time Voltage Stability Index

Yanfeng Gong and Noel Schulz, *Mississippi State University*  
 Armando Guzmán, *Schweitzer Engineering Laboratories, Inc.*

**Abstract**—This paper presents a new online voltage stability index (VSI) that predicts the power system steady-state voltage stability limit. Starting with deriving a method to predict three types of maximum transferable power (real power, reactive power, and apparent power) of a single-source power system, a new VSI based on the calculated load margins is devised. In order to apply the VSI to large power systems, a method is developed to simplify the large network behind a load bus into a single source and a single transmission line using time-synchronized phasor measurements and network parameters. The simplified system model, to which the devised VSI can be applied, preserves power flow and voltage information of the particular load bus under study. The proposed VSI combined with the network simplification method provides the voltage stability margin of each individual load bus in an informative format and identifies the load bus that is the most vulnerable to voltage collapse. Test results from applying the VSI on two test systems validate its applicability for online applications.

## I. INTRODUCTION

In recent years, power systems have operated closer to their stability limits because new power system infrastructure construction has lagged behind the steady increment of electricity demand and the increasing practice of long distance bulk power transmission. If the load demand is beyond the maximum power limit (active power and reactive power) that can be generated and transferred from the source to the load area, and no remedial actions are taken, the load area voltages will become unstable and even collapse. Power system voltage collapse or instability is a dynamic phenomenon involving many nonlinear devices. The time scale of voltage collapse could range from seconds to hours [1].

One method to effectively prevent voltage collapse requires an efficient online voltage stability assessment method in addition to a good offline system planning practice, which is normally limited to a small number of operational conditions and contingencies as compared to all possible contingencies. Utilities use dynamic simulations and steady-state analysis for voltage stability assessment. Dynamic simulations calculate system voltages in response to a sequence of events and help to identify potential voltage problems in the system based on proper modeling of generators, excitation systems, static Var compensators (SVCs), etc. Although the quasi-steady-state (QSS) modeling technique combined with the new computer simulation software can reduce simulation time, dynamic simulations are still time consuming for online applications and, therefore, are limited to offline study and verification of the corrective strategies designed to improve voltage stability. Numerous static analysis-based voltage stability indices

(VSIs) have been developed to determine power system voltage stability margins. Power flow analysis-based VSIs, such as Jacobian matrix singular values [3][4][5] and load flow feasibility [6][7], are not suitable for online applications because power flow calculations inherently depend on traditional state estimators, which normally take minutes to update the snapshot of the power systems. Because direct measurement-based VSIs, such as bus voltage ( $V$ ) and sensitivity factors ( $\frac{\partial V}{\partial Q}$  or  $\frac{\partial V}{\partial P}$ ) are simpler than the above approaches, utilities are implementing them in protection devices to prevent voltage collapse [8][9][10]. However, these existing measurement-based VSIs have difficulty accurately identifying the system voltage stability margins. For initiating remedial actions, the optimal pickup values of these direct measurement-based VSIs are difficult to determine. The local measurement-based voltage instability predictor (VIP) in [11] predicts the load bus voltage stability based on the estimated Thévenin equivalent behind the load bus. The main limitation of this method is that the Thévenin equivalent is assumed to be constant during two consecutive sets of measurements at the local load bus.

Successful commercialization of synchronized phasor measurement technology now makes it possible to build wide area monitoring systems (WAMSs), which consist of phasor measurement units (PMUs) and reliable high-speed communications networks [12][13]. A typical WAMS takes snapshots of the power system variables where the PMUs are installed, within 1 second, and provides a new platform for developing wide area stability assessment and protection applications for early detection and prevention of potential system instabilities such as voltage instabilities. The VSI presented in this paper is based on time-synchronized measurements available in WAMSs.

This paper is organized as follows. In Section II, a VSI is devised for a simple power system model. In Section III, a method is devised to simplify a large system network behind a load bus into the simple model to which the devised VSI can be easily applied. The applicability of the proposed VSI is illustrated in Section IV through simulation results from applying the VSI to two test cases. Finally, conclusions are included in Section V.

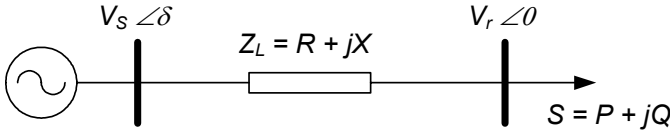


Fig. 1 A simple power system to determine VSI using  $V_s$ ,  $Z_L$ , and  $S$

## II. VSI OF A SIMPLE POWER SYSTEM

Given a simplified power system model as shown in Fig. 1, the source with voltage magnitude  $V_s$  supplies a remote load through a single transmission line with line impedance  $Z_L = R + jX$ .

The load active power,  $P$ , and reactive power,  $Q$ , can be expressed by (1) and (2), respectively. Combining these two equations by eliminating  $\delta$ , the load voltage magnitude,  $V_r$ , can be solved by (3) as a function of source voltage magnitude ( $V_s$ ), line parameters ( $R$  and  $X$ ), and load demand ( $P$  and  $Q$ ). Because the load voltage magnitude  $V_r$  is a physical quantity, there must always be a real number solution and, therefore,  $A$  in (3) must not be less than zero, as shown by (4).

$$P = \left[ (V_s \cos \delta - V_r) \frac{R}{R^2 + X^2} + V_s \sin(\delta) \frac{X}{R^2 + X^2} \right] V_r \quad (1)$$

$$Q = \left[ (V_s \cos \delta - V_r) \frac{X}{R^2 + X^2} - V_s \sin(\delta) \frac{R}{R^2 + X^2} \right] V_r \quad (2)$$

$$V_r = \sqrt{\frac{V_s^2}{2} - (QX + PR) \pm \sqrt{A}} \quad (3)$$

$$\text{where, } A = \frac{V_s^4}{4} - (QX + PR)V_s^2 - (PX - QR)^2$$

$$A \geq 0 \quad (4)$$

(4) designates the maximum transferable power  $S_{max} = P + jQ$  through this transmission line, given a source with voltage magnitude,  $V_s$ . When the equal condition of (4) is true, there is only one possible solution of  $V_s$ , and the load voltage is at the marginally stable operating point because the load demand has reached the maximum transferable power through this transmission line from the source.

With time-synchronized measurements of source voltage magnitude,  $V_s$ , and load demand  $S = P + jQ$ , the maximum active power demand,  $P_{max}$ , can be calculated by (5), where  $|Z_L| = \sqrt{R^2 + X^2}$ , assuming that the load reactive power demand  $Q$  is constant. Similarly, maximum reactive power demand  $Q_{max}$  and maximum complex power demand  $S_{max}$  can be calculated with (6) and (7), assuming the active power demand,  $P$ , and the load power angle,  $\theta = \arctan\left(\frac{Q}{P}\right)$  are constant, respectively. For transmission lines with a high  $\frac{X}{R}$  ratio, the approximate  $P_{max}$ ,  $Q_{max}$ , and  $S_{max}$  can be expressed by (8) – (10), neglecting the line resistance  $R$ .

$$P_{max} = \frac{QR}{X} - \frac{V_s^2 R}{2X^2} + \frac{|Z_L| V_s \sqrt{V_s^2 - 4QX}}{2X^2} \quad (5)$$

$$Q_{max} = \frac{PX}{R} - \frac{V_s^2 X}{2R^2} + \frac{|Z_L| V_s \sqrt{V_s^2 - 4PR}}{2R^2} \quad (6)$$

$$S_{max} = \frac{V_s^2 \left[ |Z_L| - (\sin(\theta)X + \cos(\theta)R) \right]}{2(\cos(\theta)X - \sin(\theta)R)^2} \quad (7)$$

$$P_{max} = \sqrt{\frac{V_s^4}{4X^2} - Q \frac{V_s^2}{X}} \quad (8)$$

$$Q_{max} = \frac{V_s^2}{4X} - \frac{P^2 X}{V_s^2} \quad (9)$$

$$S_{max} = \frac{(1 - \sin(\theta)) V_s^2}{2 \cos(\theta)^2 X} \quad (10)$$

It is noted that the three predicted maximum transferable powers increase as the source voltage magnitude,  $V_s$ , increases or the line impedance,  $Z_L$ , decreases. Also,  $P_{max}$  decreases as  $Q$  increases, and  $Q_{max}$  decreases as  $P$  increases.

With the predicted  $P_{max}$ ,  $Q_{max}$ , and  $S_{max}$ , three load margins ( $P_{margin}$ ,  $Q_{margin}$ , and  $S_{margin}$ ) can be readily calculated with (11) – (13), respectively. The devised VSI based on the predicted load margin is shown in (14). Smaller values of VSI indicate that the load bus is close to its voltage marginally stable operating point as less load margin is left. Once a load bus has reached its voltage marginally stable operating point, its VSI will be equal to zero.

$$P_{margin} = P_{max} - P \quad (11)$$

$$Q_{margin} = Q_{max} - Q \quad (12)$$

$$S_{margin} = S_{max} - S \quad (13)$$

$$VSI = \min \left( \frac{P_{margin}}{P_{max}}, \frac{Q_{margin}}{Q_{max}}, \frac{S_{margin}}{S_{max}} \right) \quad (14)$$

## III. VSI OF A LARGE POWER SYSTEM

Large interconnected power systems normally can be partitioned into three subsystems: the internal system (system of interest), the boundary system (buffer system), and the external system (equivalent system), as illustrated by Fig. 2(a), to facilitate analysis [14][15]. The boundary system is selected so that the effects of disturbances in the external system upon the internal system are minimized. The boundary system can be properly established through offline contingency analysis or sensitivity analysis [16]. For example, long transmission lines connecting two areas serve as good candidates for the boundary system. The external system can be approximated by modeling the remote boundary buses as PV buses, as illustrated in Fig. 2(b), without sacrificing much accuracy.

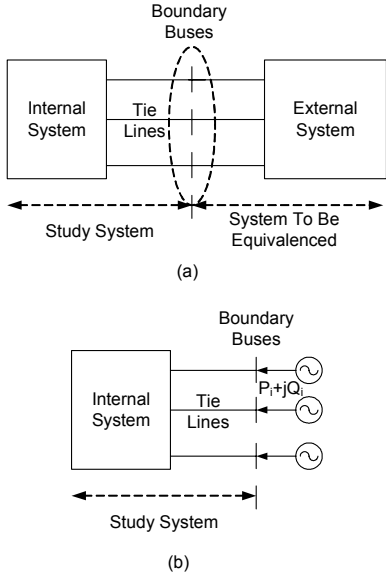


Fig. 2 (a) Interconnected power system partitioned in three systems: internal, boundary, and external (b) An equivalent system replaces the external system

The buses in the internal system can be classified into one of three categories: load bus, tie bus, and source bus. Load buses have load connected to them. A tie bus is a bus without load or any power generation device connected to it. Source buses include generator buses whose voltages are regulated by their connected generators, and boundary buses. A generator bus becomes a load bus if its connected generator reaches its capacity limit and loses its voltage regulation capability. Determination of whether a generator reaches its capacity limit can be achieved either by an indication signal from the generator overexcitation limiter (OXL) or by detecting that the generator terminal voltage is below the regulated value for a defined period of time. A boundary bus becomes a load bus if the power flow direction switches from import to export.

Injection currents into the three types of buses can be generally expressed by (15), where currents and voltages are complex numbers. In (15), the subscript  $L$ ,  $T$ , and  $G$  stand for load bus, tie bus, and source bus, respectively. The  $Y$  matrix is known as the system admittance matrix that can be constructed from the network topology and network parameters. From (15), the load bus voltages can be solved by (16) as a function of the injection currents to the load buses, the injection currents to the tie buses, the voltages of source buses, and the submatrices of the system admittance matrix.

$$\begin{bmatrix} i_L \\ i_T \\ i_G \end{bmatrix} = \begin{bmatrix} Y_{LL} & Y_{LT} & Y_{LG} \\ Y_{TL} & Y_{TT} & Y_{TG} \\ Y_{GL} & Y_{GT} & Y_{GG} \end{bmatrix} \begin{bmatrix} v_L \\ v_T \\ v_G \end{bmatrix} \quad (15)$$

$$v_L = Z_{LL}i_L + Z_{LT}i_T + H_{LG}v_G \quad (16)$$

$$\text{where, } Z_{LL} = (Y_{LL} - Y_{LT}Y_{TT}^{-1}Y_{TL})^{-1} \quad (17)$$

$$Z_{LT} = -Z_{LL}Y_{LT}Y_{TT}^{-1} \quad (18)$$

$$H_{LG} = Z_{LL}(Y_{LT}Y_{TT}^{-1}Y_{TG} - Y_{LG}) \quad (19)$$

Because the injection currents to the tie buses are zero, the voltage of the  $j^{\text{th}}$  load bus can be calculated from (20), where  $N$  is the number of load buses and  $M$  is the number of source buses. Replacing the injection currents with the complex powers flowing out of the buses, the voltage of the  $j^{\text{th}}$  load bus can be expressed by (21), where  $*$  stands for the complex number conjugate operator.

$$v_{Lj} = \sum_{i=1}^N Z_{LLji}i_{Li} + \sum_{k=1}^M H_{LGjk}v_{Gk} \quad (20)$$

$$v_{Lj} = Z_{LLjj} \left( \frac{-S_{Lj}}{v_{Lj}} \right)^* + \sum_{i=1, i \neq j}^N Z_{LLji} \left( \frac{-S_{Li}}{v_{Li}} \right) + \sum_{k=1}^M H_{LGjk}v_{Gk} \quad (21)$$

(21) can be further rearranged into (22), where the source voltage,  $V_{equ_j}$ , and line impedance,  $Z_{equ_j}$ , of the equivalent system are shown in (23) and (24), respectively. (22) represents the power flow calculation of an equivalent simple system model as shown in Fig. 1.

$$\left( \frac{v_{equ_j} - v_{Lj}}{Z_{equ_j}} \right)^* v_{Lj} = S_{Lj} \quad (22)$$

$$v_{equ_j} = \sum_{k=1}^M H_{LGjk}v_{Gk} + \sum_{i=1, i \neq j}^N Z_{LLji} \left( \frac{-S_{Li}}{v_{Li}} \right)^* \quad (23)$$

$$Z_{equ_j} = Z_{LLjj} \quad (24)$$

It is noted that the equivalent voltage source  $V_{equ_j}$  of the  $j^{\text{th}}$  load bus is a function of voltage sources and other system loads. In (23), the magnitude of the equivalent source voltage,  $V_{equ_j}$ , decreases as other system load demands increase. In (23), the equivalent impedance,  $Z_{equ_j}$ , depends on the system topology, line characteristics, and bus type status. If there is no change in network topology and bus type, the equivalent impedance remains unchanged. With the equivalent circuit parameters calculated by (23) and (24), the load margins and VSI of the  $j^{\text{th}}$  load bus can be calculated by directly applying the method presented in Section II. The VSI of the system is defined by (25), where  $L$  is the number of the load bus in the internal system. As voltage instability normally starts from local areas, different load buses may have different VSIs. The load bus with the lowest VSI has the smallest load margin and, therefore, is the closest to voltage collapse.

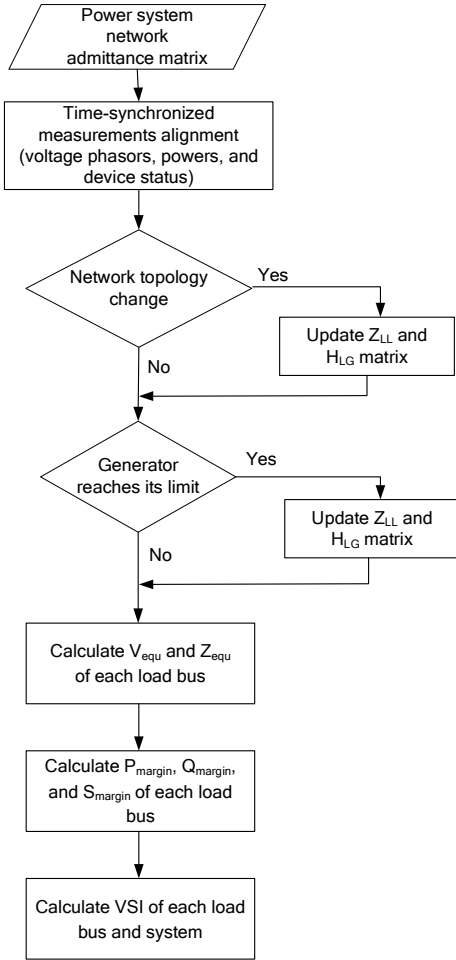


Fig. 3. Functional diagram of the VSI implementation using time-synchronized measurements

$$VSI_{sys} = \min_{i \in L} \{VSI_i\} \quad (25)$$

Fig. 3 shows the function diagram of the proposed VSI implementation. The required time-synchronized measurements include the voltage phasors of the source buses and the load buses, the complex powers or the injection currents of the source buses and the load buses, and the device statuses that are included in the network admittance matrix.

#### IV. SIMULATION RESULTS OF APPLYING VSI ON POWER SYSTEMS

This section illustrates the performance of applying the proposed VSI to two power systems. The first test system, as shown in Fig. 6, is a ten-bus multimachine system, which has been widely used to illustrate the voltage instability mechanism and to test various algorithms [2][17]. The system exhibits voltage instability after one of its 500 kV transmission lines is opened at 5 seconds, followed by under-load tap changer (ULTC) operation with 5 seconds delay between each tap change. The calculated maximum power transfer limits of both load buses (7 and 10) shrink significantly after one transmission line is opened at 5 seconds, as shown in Fig. 7 and Fig. 8. Meanwhile, the VSIs of both load buses become less than 0.1, which indicates that small load margins are left and load bus voltages are very close to the marginally stable

operating point. After the line outage, the ULTC transformer secondary voltage is below its starting threshold and, therefore, it automatically starts to change its tap position to restore the voltage of Bus 10. After seven more tap-change operations, both load buses reach their voltage marginally stable operating points at 40 seconds as their corresponding VSIs approach zero. After passing the voltage marginally stable operating point, both bus voltages start to drop dramatically, as shown in Fig. 4, and eventually collapse. If a simple VSI-based ULTC tap changer blocking scheme with VSI pickup value set at 0.05 were in place, the voltage collapse could have been prevented, as demonstrated by the steady bus voltages shown in Fig. 5.

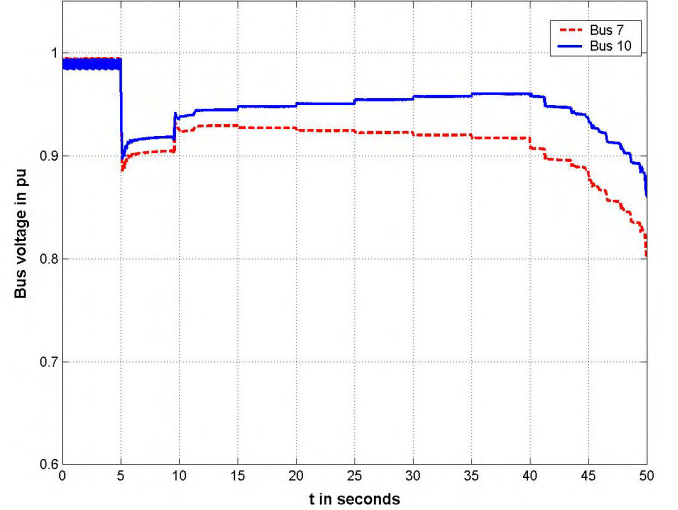


Fig. 4. Load bus (7 and 10) voltages

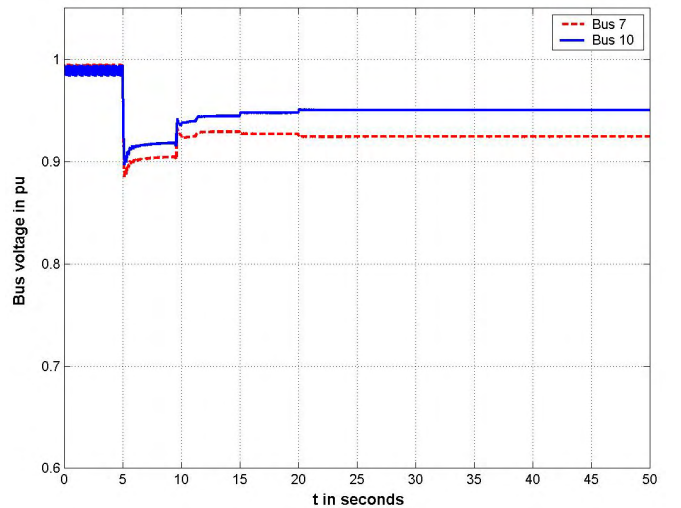


Fig. 5. Load bus voltages with a VSI-based ULTC block scheme in place

The proposed VSI is also tested on the IEEE 30-bus test system, as shown in Fig. 9 [18]. Two scenarios are simulated to demonstrate the performance of the VSI. In the first scenario, the load at Bus 10, which is not the most electrically distant load bus from the source, is increased with a constant power factor until the power flow calculation with 0.001 MW and 0.001 MVar convergence tolerance does not converge. In the second scenario, all the loads are increased simultaneously in the same percentage of their initial load values until the

power flow calculation does not converge. Fig. 10 and Fig. 11 show the VSIs of the three load buses with minimum VSI values when the power flow diverges in the two test scenarios, respectively. The results from both scenarios show that the power flow calculation diverges when the system VSI reaches the stability limit,  $VSI = 0$ . Power flow divergence is also an indication that the system has reached its maximum loading

point and voltage is at the marginally stable operating point. Fig. 10 also shows that VSI accurately identifies Load Bus 10, causing the system voltage collapse in the first scenario. In the second scenario, Load Bus 30 has the minimum VSI, as shown in Fig. 11, when the power flow diverges as expected because it is the most electrically distant load bus from the sources as compared with other load buses.

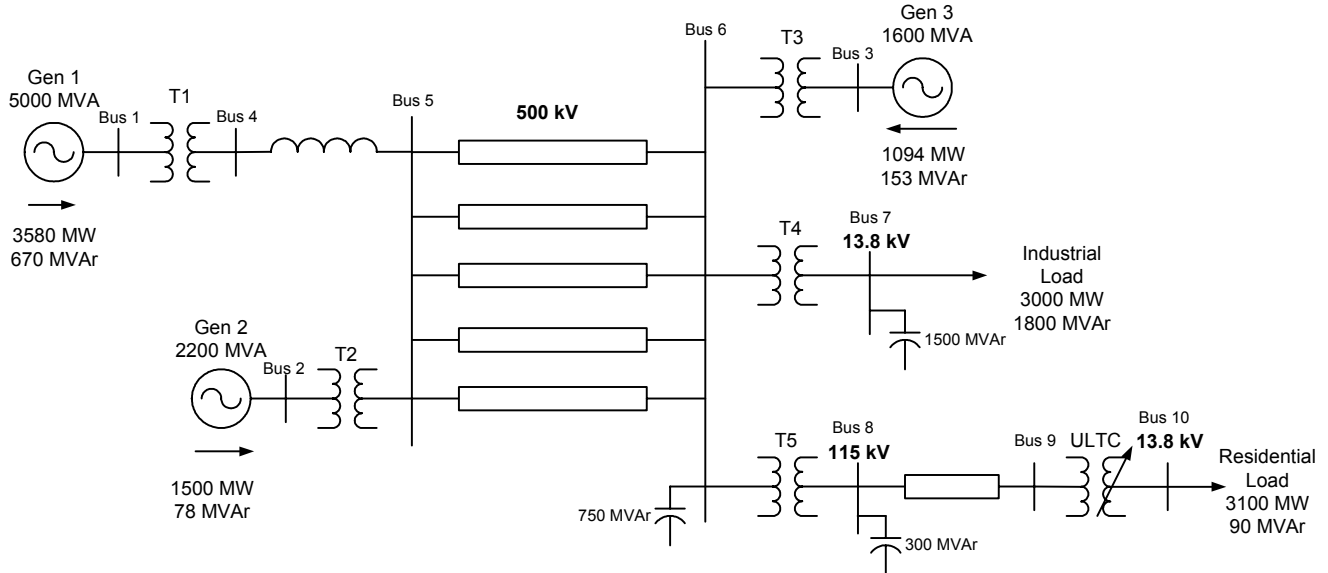


Fig. 6. A ten-bus test system for voltage stability studies [2]

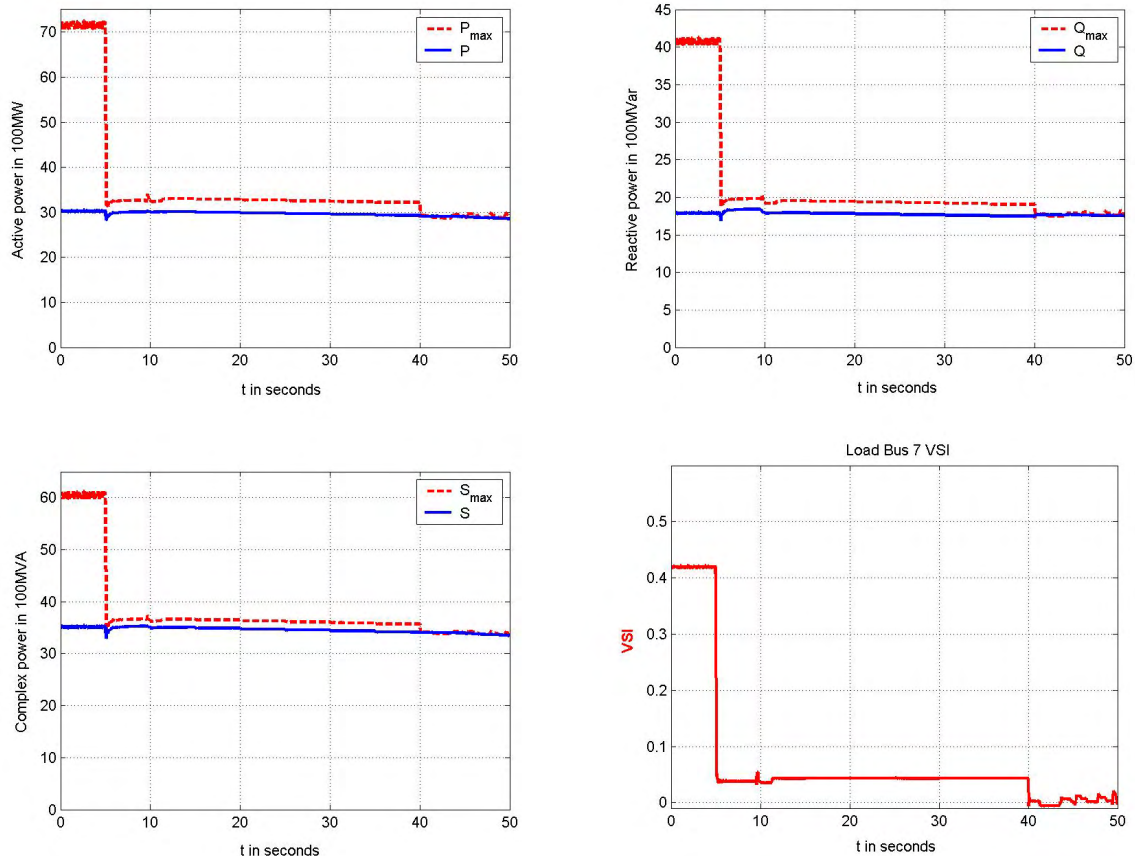


Fig. 7. Calculated maximum powers and VSI of Load Bus 7

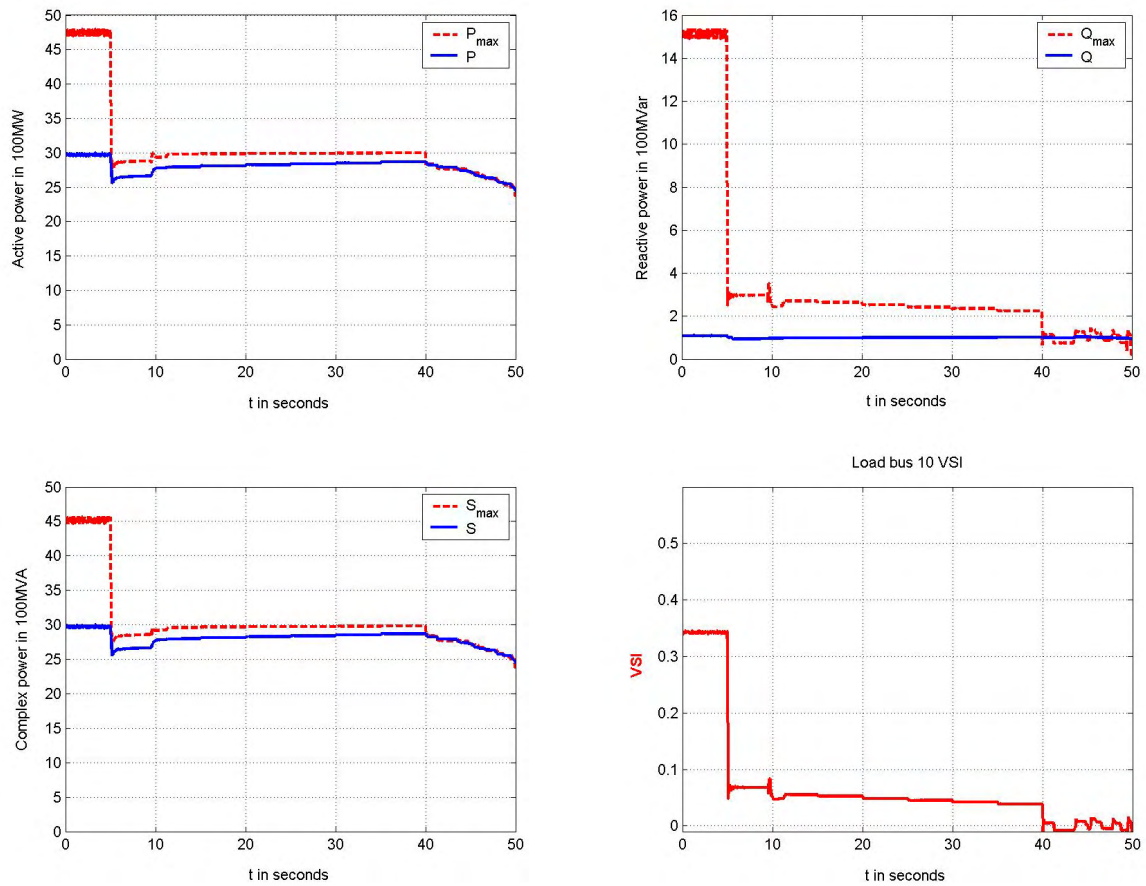


Fig. 8. Calculated maximum powers and VSI of Load Bus 10

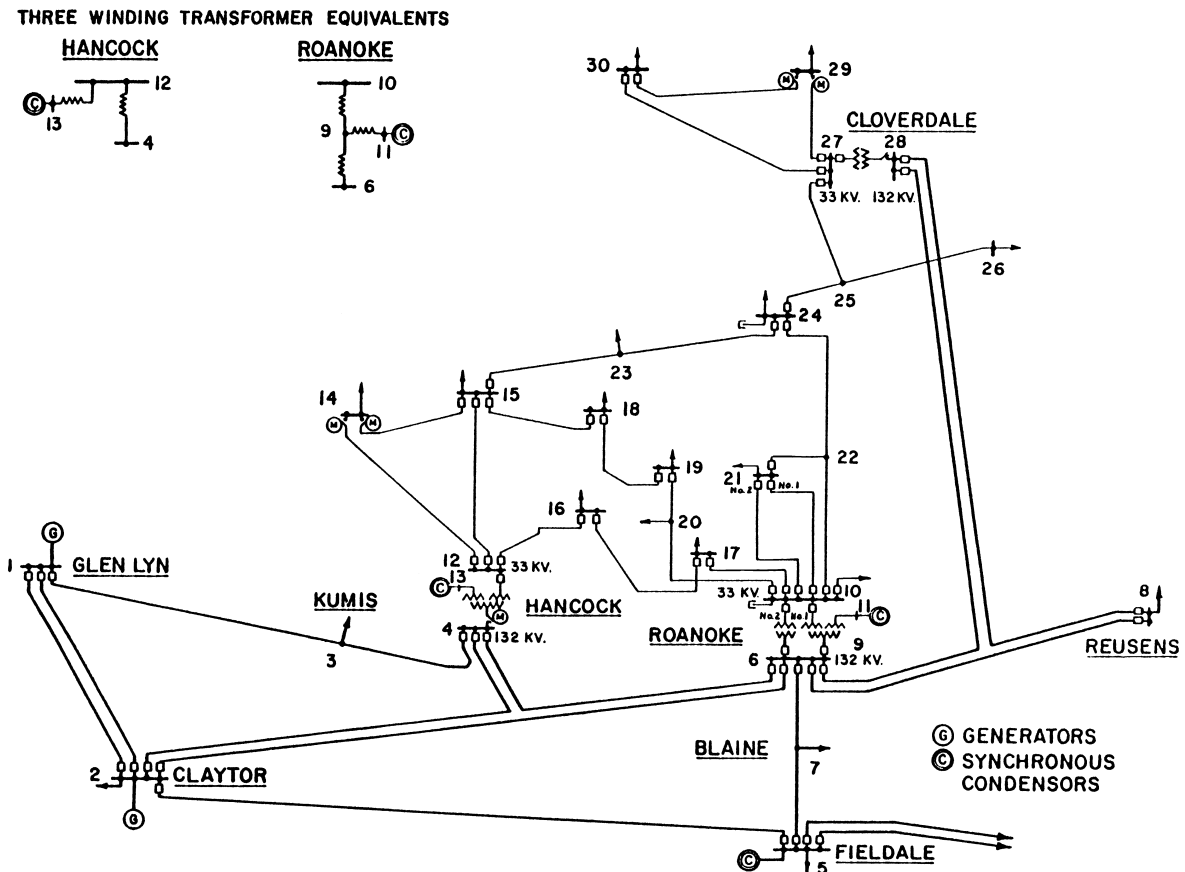


Fig. 9. IEEE 30-bus system [17]

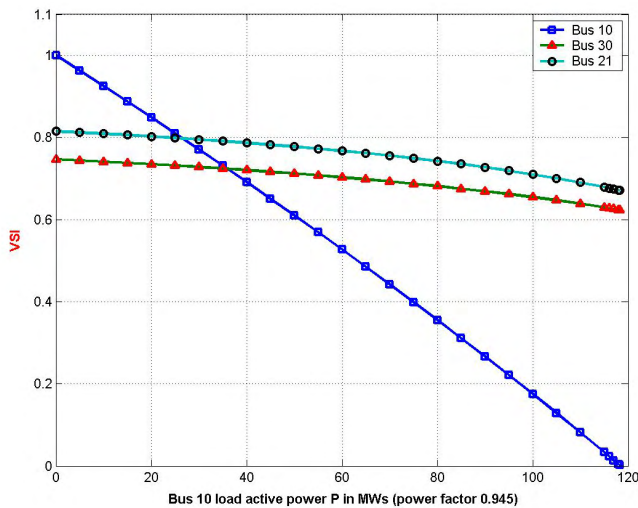


Fig. 10. At Bus 10, VSI is closer to the stability limit (VSI = 0) than the VSIs at Buses 21 and 30 in Test Scenario 1

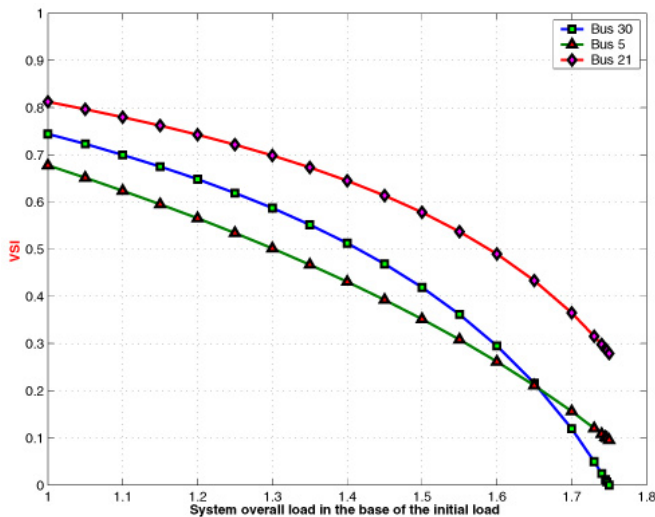


Fig. 11. At Bus 30, VSI is closer to the stability limit (VSI = 0) than the VSIs at Buses 5 and 21 in Test Scenario 2

## V. CONCLUSIONS

A new synchronized-phasor-measurement-based voltage stability index (VSI) is described in this paper. The proposed VSI determines the voltage stability margins of all system load buses. It has been demonstrated that as VSI approaches zero, the system approaches voltage collapse. The VSI output is easy to interpret and informative because it is based on the calculated load margin. The simplicity of the algorithm makes it suitable for online applications. Simulation results of applying the VSI to two power systems have demonstrated its applicability.

## VI. REFERENCES

- [1] T. Van Cutsem and C. Vournas, *Voltage Stability of Electric Power Systems*, Kluwer Academic Publishers, 1998.
- [2] C. W. Taylor, *Power System Voltage Stability*, EPRI Power System Engineering Series, McGraw Hill, 1986.
- [3] B. Gao, G. K. Morison, and P. Kundur, "Voltage Stability Evaluation Using Modal Analysis," *IEEE Transaction on Power Systems*, Vol. 7, No. 4, November 1992.

- [4] C. A. Canizares, A. Z. de Souza, and V. H. Quintana, "Comparison of performance indices for detection of proximity to voltage collapse," *IEEE Transactions on Power Apparatus and Systems*, Vol. 11, No. 3, August 1996, pp. 1441–1450.
- [5] P. A. Löf, T. Smed, G. Anderson, and D. J. Hill, "Fast calculation of a voltage stability index," *IEEE Transactions on Power Systems*, Vol. 7, No. 1, February 1992, pp. 54–64.
- [6] Y. Tamura, H. Mori, and S. Iwamoto, "Relationship between voltage instability and multiple load flow solutions in electric power systems," *IEEE Transactions on Power Apparatus and Systems*, Vol. 102, No. 5, May 1983, pp. 1115–1125.
- [7] P. Kessel and H. Glavitsch, "Estimating the voltage stability of a power system," *IEEE Transactions on Power Systems*, Vol. 1, No. 3, July 1986, pp. 346–354.
- [8] C. W. Taylor, "Concept of Undervoltage Load Shedding for Voltage Stability," *IEEE Transactions on Power Delivery*, Vol. 7, No. 2, April 1992.
- [9] A. Guzmán, D. Tziouvaras, E. O. Schweitzer, and K. E. Martin, "Load and wide-area network protection system improve power system reliability," *Proceedings of 59th Annual Protective Relaying Conference*, Atlanta, Georgia, April 2005.
- [10] "Indices predicting voltage collapse including dynamic phenomena," technical report TF 38-02-11, CIGRE, 1994.
- [11] K. Vu, M. M. Begovic, D. Novosel, M. M. Saha, "Use of local measurements to estimate voltage-stability margin," *IEEE Transactions on Power Systems*, Vol. 14, No. 3, August 1999, pp. 1029–1035.
- [12] G. Benmouyal, E. O. Schweitzer, and A. Guzmán, "Synchronized Phasor Measurement in Protective Relays for Protection, Control, and Analysis of Electric Power Systems," *Western Protection Relay Conference*, 29 Annual, Spokane, WA, October 2002.
- [13] C. W. Taylor, "The Future in On-Line Security Assessment and Wide-Area Stability Control," *Proceedings of the 2000 IEEE/PES Winter Meeting*, Vol. 1, January 2000.
- [14] A. Monticelli, S. Deckmann, A. Garcia, and B. Scott, "Real-time External Equivalents for Static Security Analysis," *IEEE Transactions on Power Apparatus and Systems*, Vol. PAS-98, No. 2, March 1979, pp. 498–503.
- [15] Ken Kato, "External Network Modeling – Recent Practical Experience," *IEEE Transactions on Power Systems*, Vol. 9, No. 1, February 1994, pp. 216–225.
- [16] R. R. Shoultz and W. J. Bierck, Jr. "Buffer system selection of a steady-state external equivalent model for real-time power flow using an automated model for analysis procedure," *IEEE Transactions on Power Apparatus and Systems*, Vol. 3, No. 3, August 1988, pp. 1104–1111.
- [17] P. Kundur, *Power System Stability and Control*, EPRI Power System Engineering Series, McGraw Hill, 1994.
- [18] University of Washington Power System Test Case Archive, <http://www.ee.washington.edu/research/pstca/>.

## VII. BIOGRAPHIES

**Yanfeng Gong** is a Ph.D. candidate in the Electrical and Computer Engineering Department of Mississippi State University. He received his B.S.E.E. from Wuhan University in 1998 and his M.S.E.E. from Michigan Tech. University in 2002. Currently he is working at Schweitzer Engineering Laboratories as an associate research engineer. His current research interests are in power system stabilities, power system protection, and general computer application in power systems.

**Noel N. Schulz** received her B.S.E.E. and M.S.E.E. degrees from Virginia Polytechnic Institute and State University in 1988 and 1990, respectively. She received her Ph.D. in EE from the University of Minnesota in 1995. She has been an associate professor in the ECE department at Mississippi State University since July 2001. She is the current holder of the TVA power system professorship. Prior to that she spent six years on the faculty of Michigan Tech. Her research interests are in computer applications in power system operations, including artificial intelligence techniques. She is a NSF CAREER award recipient. She has been active in the IEEE Power Engineering Society

and is serving as Secretary for 2004–2005. She was the 2002 recipient of the IEEE/PES Walter Fee Outstanding Young Power Engineer Award. Dr. Schulz is a member of Eta Kappa Nu and Tau Beta Pi.

**Armando Guzmán** (M '95, SM '01) received his B.S.E.E. with honors from Guadalajara Autonomous University (UAG), Mexico, in 1979. He received a diploma in fiber-optics engineering from Monterrey Institute of Technology and Advanced Studies (ITESM), Mexico, in 1990, and his M.S.E.E. from University of Idaho, USA, in 2002. He served as regional supervisor of the Protection Department in the Western Transmission Region of the Federal Electricity Commission (the electrical utility company of Mexico) in Guadalajara, Mexico for 13 years. He lectured at UAG in power system protection. Since 1993, he has been with Schweitzer Engineering Laboratories in Pullman, Washington, where he is presently Research Engineering Manager. He holds several patents in power system protection and metering. He is a senior member of IEEE and has authored and coauthored several technical papers.

Previously presented at the 2006 IEEE PES  
Power Systems Conference and Exposition.

© 2006 IEEE – All rights reserved.  
20050922 • TP6224-01